Enhancement of ferromagnetism by substituting Cu for Mn in Ni-Mn-In-B Heusler alloys

Sudip Pandey[1*], Abdiel Quetz[1], Anil Aryal[1], Ahmad Us Saleheen[2], Igor Dubenko[1], Dipanjan Mazumdar[1], Shane Stadler[2], Naushad Ali[1]

[1]*Department of Physics, Southern Illinois University, Carbondale, IL 62901, USA*
[2]*Department of Physics & Astronomy, Louisiana State University, Baton Rouge, LA 70803, USA*

[*]Corresponding author, Tel: 1-618-303-8327; E-mail: sudip@siu.edu

Received: 19 September 2016, Revised: 16 October 2016 and Accepted: 03 November 2016

DOI: 10.5185/amlett.2017.1403
www.vbripress.com/aml

Abstract

The effects of substituting Cu for Mn on the magnetocaloric, transport, and thermomagnetic properties of $Ni_{50}Mn_{35-x}Cu_xIn_{14}B$ (x = 0, 1.25, 2.0) Heusler alloys were studied. It has been found that the magnitude of the magnetization jump at the martensitic transformation decreased with increasing Cu concentration. Smaller magnetic entropy changes (ΔS_M) were observed for the alloys with higher Cu concentrations. A decrease in the resistivity was observed with increasing Cu concentration. The magnetoresistance was dramatically suppressed with increasing Cu concentration due to the weakening of the antiferromagnetic (AFM) interactions in the martensitic phase. The experimental results demonstrate that Cu in $Ni_{50}Mn_{35-x}Cu_xIn_{14}B$ Heusler alloys suppresses the AFM interactions and enhances the ferromagnetic (FM) interactions in these alloys. Possible mechanisms responsible for the observed behavior are discussed. Copyright © 2017 VBRI Press.

Keywords: Heusler alloys, ferromagnetism, magnetoresistance, magnetocaloric effects.

Introduction

The Mn-based full-Heusler alloys have drawn significant interest in recent years due to their unique magnetic properties that can be utilized in energy related applications **[1, 2]**. These stoichiometric Heusler alloys are ternary intermetallic compounds with the composition X_2YZ in which X and Y are 3d elements and Z is a group IIIA to VA element. Among these compounds, the Ni-Mn-In based alloys exhibit multiple transitions: (i) a low-temperature transition from a ferromagnetic to antiferromagnetic or paramagnetic phase at the Curie temperature of the martensitic phase (T_{CM}), (ii) from a low magnetic state (antiferromagnetic/paramagnetic) of the martensitic phase to a ferromagnetic austenitic phase at the martensitic transition temperature T_M, and (iii) from a ferromagnetic austenitic phase to a paramagnetic austenitic at the Curie temperature of the austenitic phase at T_C **[3-7]**. The first-order structural transitions of the martensitic phase at T_M in off-stoichiometric Ni–Mn–In alloys can be accompanied by a sharp change in magnetization and multiple magnetic states that often result in pronounced phenomena such as giant normal and inverse (negative) magnetocaloric effects **[8-10]**, large magnetoresistance **[11, 12]**, giant Hall effects **[13]**, and shape memory effects **[14]**.

It has been suggested that the specific features of electronic band structure of the Heusler alloys are responsible for the magnetostructural transition (MST) **[15]**. The phase transition temperatures and types of magnetic ordering of the different structure modifications are extremely sensitive to the alloys' electronic structures and therefore depend strongly on the chemical compositions. Therefore, the alloy composition, the concentration of valence electrons per atom (e/a), interatomic distances, and crystal structure homogeneity are interconnected major factors affecting the phase transitions and the related phenomena. It has been discovered that the Ni-Mn-In-B systems show an asymmetric resistance switching in small magnetic fields, i.e., a large low-field magnetoresistance (MR) **[16, 17]**. It has also been shown that Ni-Mn hybridization is a major factor determining the magnetic properties, especially antiferromagnetic (AFM) interactions in the martensitic state **[18]**. Therefore, a stronger Ni-Mn hybridization result in the suppression of ferromagnetism. The partial substitution of Mn by Cr in $Ni_{50}Mn_{37-x}Cr_xSb_{13}$ Heusler alloys shows in the destabilization of the martensitic phase due to the weakening of Ni-Mn hybridization **[19]**.

Recently, we studied the influence of small compositional changes through the substitution of In by isoelectronic B in $Ni_{50}Mn_{35}In_{15}$ alloys, and it has been found that the concentration dependences of the MST can be explained by the decrease in crystal cell volume and distortion of the local atomic environment **[20]**. It was reported that the MST (T_M) increases with increasing pressure in NiCoMnSb Heusler alloys **[21]**. Hence to explore the effects of pressure on the transition temperatures and to observe the change in the magnetic and magnetocaloric properties through the small

compositional changes, we report the experimental investigations on Ni-Mn-In Heusler alloys. Here, we try to optimize the Heusler series Ni–Mn–In-B to explore how the magnetic properties of this alloys change with the Cu substitution.

In this work, experimental studies of magnetic, magnetocaloric, and magnetotransport, properties have been carried out for $Ni_{50}Mn_{35-x}Cu_xIn_{14}B_1$ Heusler alloys. The experimental results reveal an enhancement of ferromagnetism through the substitution of Cu for Mn in the $Ni_{50}Mn_{35-x}Cu_xIn_{14}B_1$ alloys.

Experimental techniques

Bulk polycrystalline samples of $Ni_{50}Mn_{35-x}Cu_xIn_{14}B_1$ (x=0, 1.25, and 2.0) were prepared by arc-melting under the constant flow of "ultra-high" purity argon using a water-cooled bronze crucible and tungsten electrode. The samples were re-melted more than four times to establish homogeneity. The difference in mass before and after melting may be due to the loss of Mn because of the high volatility of Mn compared to other components, an amount of Mn of about 1 wt. % of the total sample mass was added to compensate for Mn loss during melting **[22]**. The melted samples were annealed in high vacuum (~ 10^{-5} torr) at 850°C for 48 hrs. The magnetic properties were measured at temperatures ranging from 5-400 K and in magnetic fields up to 5 T using a Quantum Design superconducting quantum interference device magnetometer (SQUID). The resistance and magnetoresistance (MR) of the samples were measured using the four-probe method in the temperature interval 5 - 400 K and in magnetic fields up to 5 T. In the measurements under hydrostatic pressure, Daphne (7373) oil was used as the pressure-transmitting medium and the value of the applied pressure was calibrated by measuring the shift of the superconducting transition temperature of Pb used as a reference manometer (T_C~7.2 K at ambient pressure). The differential scanning calorimetry (DSC) measurements were carried out employing a Perkin-Elmer DSC 8000 instrument (with the ramp rate of 20 K/min during heating and cooling) in the temperature range of 123-473 K.

Results and discussion

The temperature dependence of the magnetization, or M(T) curves for $Ni_{50}Mn_{35-x}Cu_xIn_{14}B_1$ (x=0, 1.25, and 2.0) measured during heating and cooling, in the presence of magnetic field of 100 Oe is shown in **Fig. 1(a)**. All of the compounds show a thermal hysteresis in magnetization during cooling and heating. The presence of hysteresis and the jump-like change in magnetization signifies first order structural (martensitic) transitions. For all of the alloys, a first order magnetostructural transition (MST) from a ferromagnetic austenitic (FA) to low magnetic moment state (antiferromagnetic martensitic (AFM) or paramagnetic martensitic (PM)) and a second order transition from a paramagnetic austenitic (PA) to a ferromagnetic austenitic (FA) phase was observed. Splitting of the zero-field-cooled (ZFC) and field- cooling (FC) magnetization curve was observed for the alloy with x=0 slightly above the blocking temperature (T_B) which is evidence of the exchange bias phenomena **[23, 24]**. It was suggested that this type of behavior in bulk Heusler alloys arises from the presence of both AFM and FM fractions in the systems **[25]**.

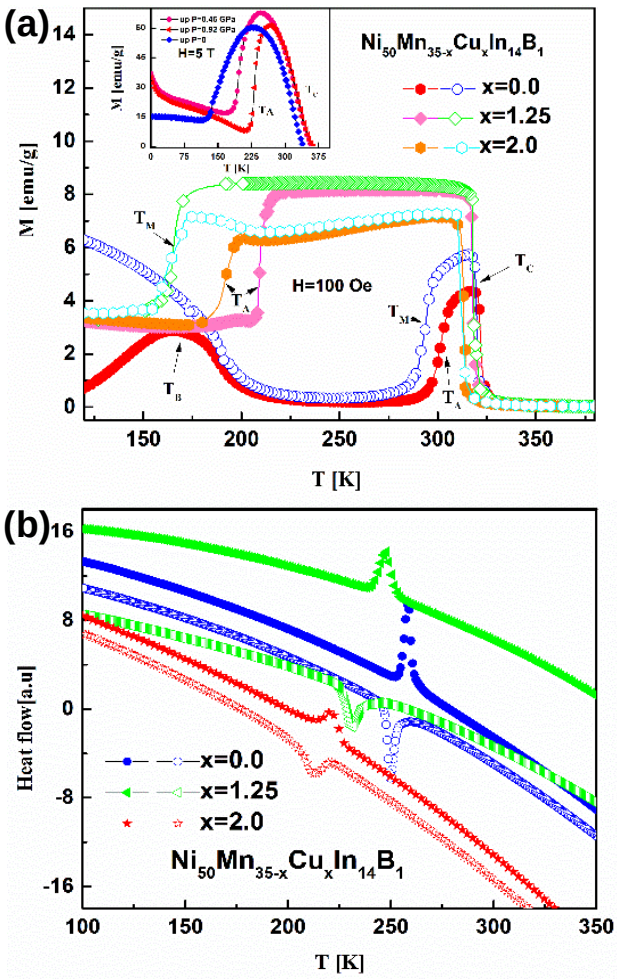

Fig. 1. (a) Temperature dependence of the magnetization in the presence of a 100 Oe magnetic field during heating and cooling for $Ni_{50}Mn_{35-x}Cu_xIn_{14}B_1$. The inset shows the M(T) curves of $Ni_{50}Mn_{33.75}Cu_{1.25}In_{14}B_1$ obtained at H = 5 T for different applied pressures (P). (b) DSC heat flow curves as a function of temperature measured at a rate of 20K/min during heating and cooling.

The partial substitution of Cu shifts both the martensitic transition temperature (T_M) and Curie temperature (T_C) to lower temperatures. A change of Cu concentration from x=0 to 1.25 results in a shift of the MST from 300 K to 215 K, as determined from the maximum change of temperature dependent dM/dT in the magnetization heating curve. From **Fig. 1(a)**, we can see that the magnitude of the magnetization jump at the martensitic transformation decreased with increasing Cu concentration. The change in magnetization at the martensitic transition temperature is related to the suppression of antiferromagnetic (AFM) interactions of the martensitic phase for Mn rich Heusler alloys **[26]**. The inset of **Fig. 1(a)** shows the M(T) curve of $Ni_{50}Mn_{33.75}Cu_{1.25}In_{14}B_1$ obtained at magnetic field of 5 T

for different applied pressures P. The application of external pressure results in a substantial shift in the martensitic transition temperature towards higher temperature and a weak increase in T_C with $\Delta T_M/\Delta P$ = 98.5 K/GP and $\Delta T_C/\Delta P$ = 3.4 K/GP. Hence the application of hydrostatic pressure increases the temperature stability of the martensitic phase. Our results are also consistent with those reported for Ni-Co-Mn-Sb Heusler alloys **[21]**.

The first-order MST was also observed in the DSC measurements which are shown in **Fig. 1(b)**. The well-defined endothermic/exothermic peaks, observed during heating/cooling cycles, are related to the latent heat of the first-order magnetostructural transition from low magnetization to the ferromagnetic structure. The temperature hysteresis of the heat flow of about 18 K between heating and cooling cycles detected from DSC measurements are consistent with the magnetization results. A broad maximum in the heat flow has been detected for all of the samples. The exothermic and the endothermic peaks shift toward thelower temperature with increasing in Cu concentration. Hence, we can see that the first order transition temperature decreases with increasing in Cu concentration.

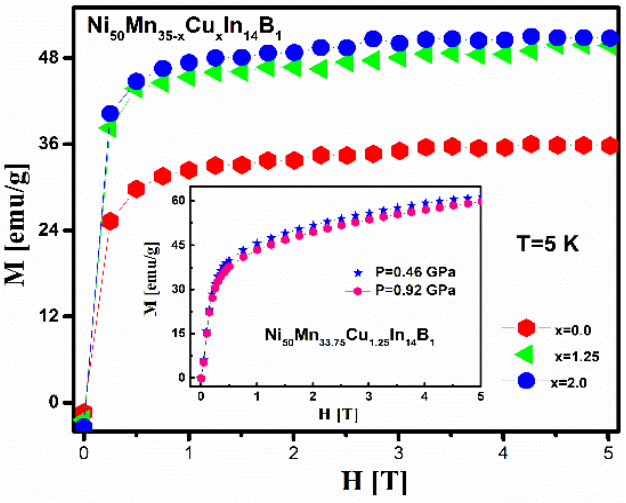

Fig. 2. Magnetization (M) as a function of magnetic field (H), at T = 5 K. The inset shows M as a function of H for different applied pressures (P).

The field dependence of the magnetization M(H) curves of $Ni_{50}Mn_{35-x}Cu_xIn_{14}B_1$ (x=0, 1.25, and 2.0) at 5 K are shown in **Fig. 2**. All of the compounds were found to exhibit the ferromagnetic type behavior. The saturation field was observed to increase for increasing Cu concentration (see **Fig. 2**). Also, the saturation magnetization at 5 K increased linearly with the increasing Cu concentration which demonstrates an enhancement of ferromagnetic (FM) interactions and a suppression of AFM interactions. The M(H) curves obtained under the application of applied hydrostatic pressure at 5 K for $Ni_{50}Mn_{33.75}Cu_{1.25}In_{14}B_1$ are shown in the inset of **Fig. 2**. The magnetization was found to increase under the application of pressure. Hence, the M(H) curves obtained under applied pressure demonstrate behavior consistent with a non-collinear ferromagnetic state with a weak tendency for saturation in magnetic fields.

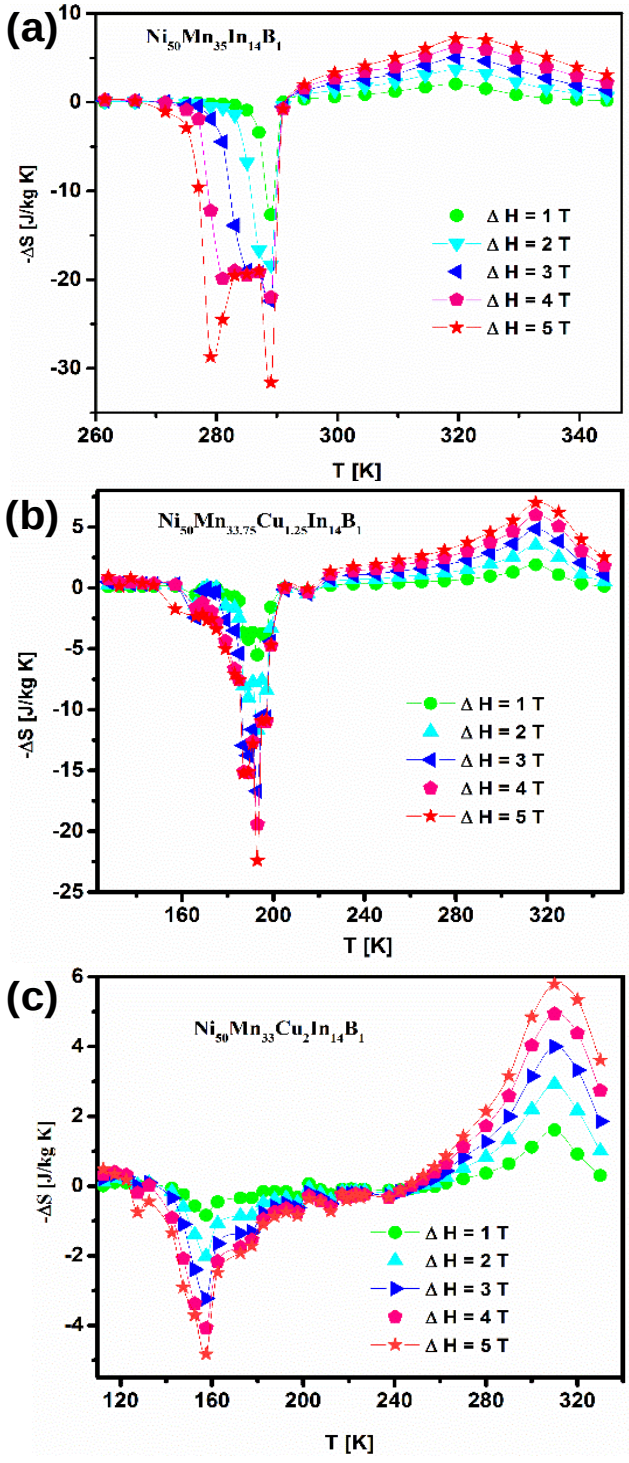

Fig. 3. Magnetic entropy changes (ΔS_M) as a function of temperature for (a) $Ni_{50}Mn_{35}In_{14}B_1$, (b) $Ni_{50}Mn_{33.75}Cu_{1.25}In_{14}B_1$, and (c) $Ni_{50}Mn_{33}Cu_2In_{14}B_1$.

The magnetic entropy changes, ΔS_M, as a function of temperature for the various applied fields (ΔH) are shown in **Fig. 3.** The $\Delta S_M(T, H)$ was estimated from the isothermal magnetization curves near the martensitic/

magnetic transition temperature using the Maxwell relation **[27]**.

$$\Delta S_M = \int_0^H \left(\frac{\partial M}{\partial T}\right) H dH$$

At the FOT, $Ni_{50}Mn_{35}In_{14}B_1$ exhibits a large positive ΔS_M of 32 $J \cdot kg^{-1} \cdot K^{-1}$ (at T = 290K) (see **Fig. 3 (a)**), and a negative ΔS_M of 6.6 $J \cdot kg^{-1} \cdot K^{-1}$ in the vicinity of the SOT in a magnetic field changes of 5 T. These values of ΔS_M are higher than that obtained from Ag doped Ni-Mn-In Heusler alloys **[28]**. The splitting of the ΔS_M curves into two maxima were observed for the samples with x= 0 and 1.25. The low temperature maximum of ΔS_M may have originated from an arrested austenitic phase, i.e., from magnetic cycling during the reverse field-induced MST **[29]**.

With the increase in Cu concentration, ΔS_M at both the FOT and SOT decrease significantly (see **Fig. 3 (b)** and **Fig. 3 (c)**). The small value of ΔS_M at the FOT could be due the fact that martensitic transition is not as sharp as in the parent alloy. The magnitude of the magnetization change decreased dramatically with increasing the Cu concentration due to the enhancement of ferromagnetism (see **Fig. 1(a)**). Since, magnetocaloric effects depends on the magnitude of the magnetization change for Mn rich Heusler alloys, high values of ΔS_M can be expected where the system shows a large value of ΔM at the first order field-induced transition. This observed magnetization behavior is similar to those reported for Ni-Mn-Cr-Sb Heusler alloys where it has been detected that the suppression of antiferromagnetic interaction with increasing Cr concentration **[26]**.

The temperature dependence of the resistivity for the $Ni_{50}Mn_{35-x}Cu_xIn_{14}B_1$ alloys are shown in **Fig. 4 (a)**. Abrupt drops in the resistivity and the respective slope changes were observed for all of the alloys in the vicinities of T_M. The step-like drops of the resistivity at T_M is evidence of the first order nature of the martensitic transformation in Mn-rich Heusler alloys. The large value of the resistivity observed for martensitic phase is most likely related to a change in the electronic band structure, which alters the density of states near the Fermi surface, and therefore strongly affects the electronic transport properties of the system. As it can be seen from the **Fig. 4 (a)** the resistivity of the $Ni_{50}Mn_{35-x}Cu_xIn_{14}B_1$ alloys in the martensitic phase abruptly drops with increasing Cu concentration. This effect is similar to those observed for Ni-Mn-In-Ag and Ni-Mn-Cr-Sb Heusler alloys where the resistivity decreases with increasing doping concentration **[21, 28]**. The drop of resistivity with The shift of T_M to lower temperature upon the application of magnetic field results in a large magnetoresistance {MR =([R(H, T) – R(0,T)]/R(0,T))× 100 % }values of which are shown in **Fig. 4(b)**. For the alloy with x=0, a maximum MR values of about −27% was found at T_M. Because of the field induced structural transition from a low temperature martensitic to high temperature austenitic phase resulted in the large value of MR at T_M **[30]**. Thus, the larger the difference of magnetization between martensitic and the austenitic phases at a certain magnetic field at T_M, the larger the MR is observed. The peak MR decreased significantly with increasing Cu concentration (see **Fig. 4(b)**) due to the decrease in the magnetization at T_M (see **Fig. 1(a)**). Since the resistivity and MR in Mn-rich Heusler alloys depends on the strength of AFM interactions at T_M **[26]**, a decrease of resistivity and MR with increasing Cu concentration demonstrate the suppression of AFM interactions and the enhancement of FM interactions.

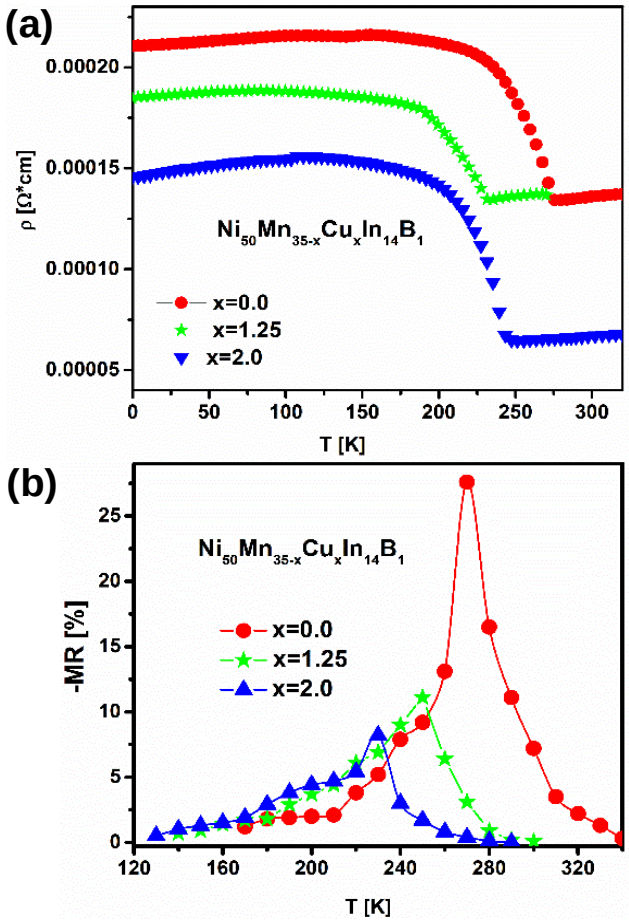

Fig. 4. (a) Temperature dependence of the resistivity for $Ni_{50}Mn_{35-x}Cu_xIn_{14}B_1$ at H=0 T. (b) Magnetoresistance for a field change of 5 T for $Ni_{50}Mn_{35-x}Cu_xIn_{14}B_1$ alloys.

Conclusion

In conclusion, the impact of Cu substitution on the magnetic, magnetocaloric, and transport properties of $Ni_{50}Mn_{35-x}Cu_xIn_{14}B_1$ Heusler alloys has been systematically studied. A shift in the martensitic transition temperature (T_M) to lower temperature was observed with the increasing Cu concentration, while the saturation magnetization at 5 K increased. The magnitude of the magnetization change decreased dramatically with increasing Cu concentration which resulted in smaller ΔS_M for the alloys with higher Cu concentrations. A decrease in resistivity and MR with increasing Cu concentration was observed due to the weakening of the antiferromagnetic interactions in the martensitic phase. Hence the effects of increasing Cu concentration revealed

a suppression of AFM interactions and an enhancement of FM interactions.

Acknowledgements

This work was supported by the Office of Basic Energy Sciences, Material Science Division of the U.S. Department of Energy DOE Grant No. DE-FG02-06ER46291 (SIU) and DE-FG02-13ER46946 (LSU).

Author's contributions

Naushad, Shane, Dipanjan, Igor, and Sudip gather the ideas and make a plan to do the experiments. Sudip, Abdiel, Anil, and Ahmad performed the experiments. Data analysis is done by Sudip. Sudip wrote the paper. Authors have no competing financial interests.

References

1. Krenke, T.; Acet, M.; Wassermann, E.; Moya, X.; Maosa, L.; Planes, A.; *Nat. Matter*., **2005**, *4*, 450. **DOI:** 10.1038/nmat1395
2. Planes, A.; Manosa, L.; Accet, M.; *J. Phys.: Condens. Matter*, **2008**, 20**,** 235204. **DOI:** 10.1088/0953-8984
3. Ito, W.; Nagasako, M.; Umetsu, R.; Kainuma, R.; Kanomata, T.; Ishida, K.; *Appl. Phys. Lett.*, **2008**, 93, 232503. **DOI:** 0.1063/1.2955839
4. Han, Z.; Wang, D.; Zhang, C.; Xuan, H.; Gu, B.; Du, Y.; *Appl. Phys. Lett.*, **2007**, 90, 042507. **DOI:** 0.1063/1.2437655
5. Quetz, A.; Koshkid'ko, Y.; Titov, I.; Rodionov, I.; Pandey, S.; Aryal, A.; Prudnikov, V.; Granovsky, A.; Dubenko, I.; Samanta, T.; Cwik, J.; Llamazares, J.; Stadler, S.; Ali, N.; J. *Alloys Comp.*, **2016**, 683,139–142. **DOI:** 10.1016/j.jallcom.2016.05.106
6. Pathak, A.; Khan, M.; Dubenko, I.; Stadler, S.; Ali, N.; *Appl. Phys. Lett.*, **2007**, 90, 262504. **DOI:** 10.1063/1.2752720
7. Dubenko, I.; Quetz, A.; Pandey, S.; Aryal, A.; Rodionov, I.; Prudnikov, V.; Lahderanta, E.; Samanta, T.; Saleheen, A.; Stadler, S.; Ali, N.; J. *Magn. Magn. Mater*., **2015**, 383,186–189. **DOI:** 10.1016/j.jmmm.2015.11.025
8. Pecharsky, A.; Gschneidner, K.; Pecharsky, V.; *J. Appl. Phys.*, **2003**, 93, 4722. **DOI:** 10.1063/1.1558210
9. Tegus, O.; Bruck, E.; Buschow, K.; Boer, F.; Nature (London), **2002**, 415, 150. **DOI:** 10.1038/415150a
10. Krenke, T.; Duman, E.; Acet, M.; Wassermann, E.; Moya, X.; Ma~nosa, L.; Planes, A.; *Nat. Mater*., **2005**, 4, 450. **DOI:** 10.1038/415150a 10.1038/nmat1395
11. Yu, S.; Liu, Z.; Liu, G.; Chen, J.; Cao, G.; Wu, H; B.; Zhang, B.; Zhang, X.; Appl. Phys. Lett., **2006**, 89, 162503. **DOI:** 10.1063/1.2362581
12. Khan, M.; Pathak, A.; Paudel, M.; Dubenko, I.; Stadler, S.; Ali, N.; *J. Magn. Magn. Mater.*, **2008**, 320, L21. **DOI:** 10.1016/j.jmmm.2007.12.019
13. Dubenko, I.; Pathak, A.; Stadler, S.; Ali, N.; Kovarskii, Ya.; Prudnikov, V.; Perov, N.; Granovsky, A.; *Phys. Rev. B*, **2009**, 80, 092408. **DOI:** 10.1103/PhysRevB.80.092408
14. Ullakko, K.; Huang, J.; Kantner, C.; Handley, R.; Kokorin, V.; *Appl. Phys. Lett.*, **1996**, 69, 1966. **DOI:** 10.1063/1.118104
15. Vasiliev, A.; Heczko, O.; Volkova, O.; Vasilchikova, T.; Voloshok, T.; Klimov, K.; Ito, W.; Kainuma, R.; Ishida, K.; Oikawa, K.; Fahler, S.; *J. D: Appl. Phys.*, **2010**, 43, 055004. **DOI:** 10.1088/0022-3727
16. Dubenko, I.; Samanta, T.; Quetz, A.; Kazakov, A.; Rodionov, I.; Mettus, D.; Prudnikov, V.; Stadler, S.; Adams, P.; Prestigiacomo, J.; Granovsky, A.; Zhukov, A.; Ali, N.; *Appl. Phys. Lett.*, **2012**, 100, 192402. **DOI:** 10.1063/1.4714539
17. Samanta, T.; Saleheen, A.; Lepkowski, D.; Shankar, A.; Dubenko, I.; Quetz, A.; Khan, M.; Ali, N.; Stadler, S.; *Phys. Rev. B*, **2014**, 90, 064412. **DOI:** 10.1103/PhysRevB.90.064412
18. Khan, M.; Jung, J.; Stoyko, S.; Mar, A.; Quetz, A.; Samanta, T.; Dubenko, I.; Stadler, S.; Ali, N.; *Appl. Phys. Lett.*, 2008, **320**, L21. **DOI:** 0.1088/0022-3727
19. Khan, M.; Pathak, A.; Paudel, M.; Dubenko, I.; Stadler, S.; Ali, N.; *J. Magn. Magn. Matter*, 2008, **320**, L21-L25. **DOI:** 10.1063/1.4705422
20. Pandey, S.; Quetz, A.; Aryal, A.; Samanta, T.; Dubenko, I.; Stadler, S.; Ali, N.; *J. Appl. Phys.*, **2015**, 117, 183905. **DOI:** 10.1063/1.4921052
21. Nayak, K. A.; Suresh, G. k.; Nigam, K. A.; Coelho, A.; Gama, S.; *J. Appl. Phys.*, **2009, 106, 053901**. **DOI:** 10.1063/1.3208064
22. Zhang, Q.; Du, J.; Li, Y.; Sun, N.; Cui, W.; Li, D.; Zhang, Z.; *J. Appl. Phys.*, **2007**, 101, 123911. **DOI:** 10.1063/1.2732073
23. Khan, M.; Dubenko, I.; Stadler, S.; Ali, N.; *Appl. Phys. Lett.*, **2007**, 102, 113914. **DOI:** 10.1063/1.2818016
24. Dubenko, I.; Khan, M.; Pathak, A.; Gautam, B.; Stadler, S.; Ali, N.; *J. Magn. Magn. Mat.*, **2009**, 321, 754. **DOI:** 10.1016/j.jmmm.2008.11.043
25. Khan, M.; Dubenko, I.; Stadler, S.; Ali, N.; *Appl. Phys. Lett.*, **2007**, 91, 072510. **DOI:** 10.1063/1.2772233
26. Khan, M.; Dubenko, I.; Jung, J.; Stoyko, S.; Mar, A.; Quetz, A.; Stadler, S.; Samanta, T.; Ali, N.; Chow, K.; *Appl. Phys. Lett.*, **2013**, 102, 112402. **DOI:** 10.1063/1.4795627
27. Tishin, A.; Spichkin, Y.; The Magnetocaloric Effects and its Applications, IOP Publishing Ltd, **2003**. **DOI:** 10.1201/9781420033373
28. Pandey, S.; Quetz, A.; Aryal, A.; Samanta, T.; Dubenko, I.; Mazumdar, D.; Stadler, S.; Ali, N.; *AIP Advances*, **2016**, 6, 056213. **DOI:** 10.1063/1.4943763
29. Dubenko, I.; Samanta, T.; Quetz, A.; Saleheen, A.; Prudnikov, V.; Granovsky, A.; Stadler, S.; Ali, N.; *Phys. Status Solidi C*, **2014,** 11, 5–6, 1000–1003. **DOI:** 10.1002/pssc.201470051
30. Yu, S.; Liu, Z.; Liu, G.; Chen, J.; Cao, Z.; Wu, G.; Zhang, B.; Zhang, X.; *Appl. Phys. Lett.*, **2006**, *89*, 162503. **DOI:** 10.1063/1.2362581